

Distribution of Magnetic Field of Linear Induction Motor

T. Sadauskas, A. Smilgevičius, Z. Savickienė

*Department of Automation, Vilnius Gediminas Technical University,
Naugarduko str. 41, LT-03227 Vilnius, Lithuania, phone: +370 5 2744754;
e-mail's: ssadass@gmail.com, asm@el.vtu.lt, zita.savickiene@el.vtu.lt*

Introduction

The magnetic field of an LIM is more complex than that of a rotating induction motor. At analysis of LIM the limited dimensions of the inductor should be considered. Therefore it is necessary to investigate the magnetic fields beyond the inductor boundaries (edge effect and end effect), and interdependencies of these fields. Because of the phenomenon of end effect, additional factors must be considered: there is a reduction of attraction force, and despite a balanced supply voltage, increased phase impedance and phase differences of leading currents.

Three-phase linear drive is used more often in industry because it is characterized by greater power and efficiency; however, connection requires a three-phase feeding network.

Single-phase drive has less efficiency, but can be utilized where there is a single-phase feeding network. Therefore, single-phase drive is more widely applied for domestic appliances; they can be used as controlled servomotors in automatic systems [1].

The single-phase linear motor is sparsely discussed in literature sources. Its magnetic field distribution with respect to time outside of inductor limits has not been delineated. Present day technology can be used to facilitate the investigative process into this problem. Using specially programmed software it is possible to simulate the phenomenon being tested, rapidly change conditions during simulation, and obtain simulation results for chosen cross-sections [2].

The main objective of this investigation is to study, using specialized software, the distribution of magnetic field of LIM within the air gap and outside of the inductor's limits in cases of three-phase asynchronous linear induction motor and single-phase linear capacitance motor.

The distribution of magnetic field in different cross-sections of the air gap (one – near to the inductor, second – near to the secondary element) is compared.

Flux density's changes under ending and middle tooth of inductor are presented.

Simulation model

In this article are investigated two (three-phase asynchronous linear induction motor and single-phase linear capacitance motor) one-sided flat-type LIM's with one inductor, secondary element and magnetic conductor (magnetic conductor are used to reduce magnetic resistance).

The capacitor motor was chosen for this experiment because the economic indicators for these motors are more favorable than those for single-phase motors with start-up winding.

There are made 6 slots in the inductor and are built in the three-phase winding in these slots, to generate the running magnetic field (in case of LCM – the inductor has eight slots within which reside two windings generating a magnetic field). This construction corresponds to a two-pole motor. The secondary element is copper with specific permeability of 56000000 S/m^2 , and a thickness of 6 mm. Air gap between the inductor and secondary element is $\delta - 0,25 \text{ mm}$. The windings of the inductor are supplied by alternating current with a frequency of 50 Hz; current of the winding density is 5000000 A/m^2 .

A simple model was chosen for this investigation because the accuracy and continuity of the simulation results depends on the complexity of the model - it depends on the number of mesh nodes where the parameters are calculated. All of the specialized software packages designed for magnetic field studies have limited quantity of mesh nodes to calculate the parameters [3]. Thus when using a complex model the mesh nodes are spread throughout the model and the most relevant areas have low mesh node density.

The model chosen for this study allowed for quite good results without losing essential information. It is possible to choose other simulation models (e.g. double-sided or otherwise constructed LIM's). There can be more slots or more poles but these changes will not influence the basic nature of the results.

Simulation of magnetic field

"Quickfield" software was used to simulate the magnetic field of LCM. This software applies the finite element method to simulate the magnetic field. To calculate the magnetic field the following formula is used:

$$\frac{\partial}{\partial x} \left(\frac{1}{\mu_y} \cdot \frac{\partial A}{\partial x} \right) + \frac{\partial}{\partial y} \left(\frac{1}{\mu_x} \cdot \frac{\partial A}{\partial y} \right) - g \cdot \frac{\partial A}{\partial t} = -j_0 + \left(\frac{\partial H_{cy}}{\partial x} - \frac{\partial H_{cx}}{\partial y} \right). \quad (1)$$

Magnetic field at different instants of time is realized by giving actual current densities to windings in the grooves (windings are supplied permanent voltage, that are equal to momentary voltages, for 100 s). Simulating magnetic field with different current densities and analyzing results in desirable cuts the characteristics family of magnetic field at different instants of time are made. Current densities in windings are choused to simulate, the rotation of supply voltages star by 360°.

Using the above-described methods, distribution of magnetic flux lines outside the inductor at different instants of time was investigated. For purposes of comparison, magnetic flux parameters were computed in the cross-section outside of the inductor next to the air gap between the inductor and the secondary element at both ends of inductor.

Also investigated: magnetic field (outside of the inductor ends) dependence on current's shift in phase differences between operating and capacitance windings. In this test, one moment in time was selected, and while changing the current shift in phase difference in the windings, magnetic flux density outside the inductor limits was measured. A characteristic grouping is formed showing the magnetic flux density's dependence on current shift in phase changes in the windings.

Air gap between the inductor and secondary element is 0,25 mm. Magnetic flux parameters were computed in different cross-sections of air gap in order to show influence of measurement position to results.

Results of simulation

Fig. 1 shows, the magnetic field distribution outside the inductor.

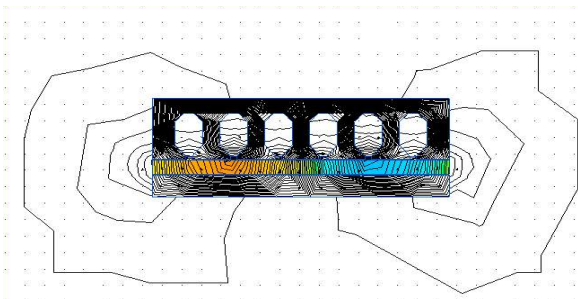


Fig. 1. Magnetic field distribution outside the inductor

Simulation, of magnetic field of three-phase asynchronous linear induction motor, show distribution of magnetic flux density in the air gap at the different instants of time (Fig. 2). It is evident, that magnetic field is running

and the magnetic flux momentary value is pulsating in all air gap long.

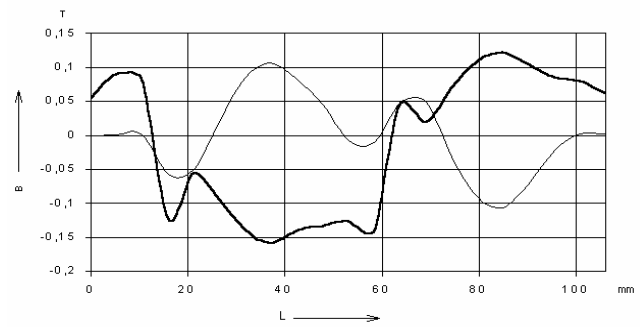


Fig. 2. Magnetic flux distribution in the air gap at the different instants of time

Simulation of magnetic field of single-phase linear capacitance motor shows that the magnetic field distribution outside of the inductor at different instances of time is also changing (Fig. 3-4), but these changing's depends on value of current shift in phase.

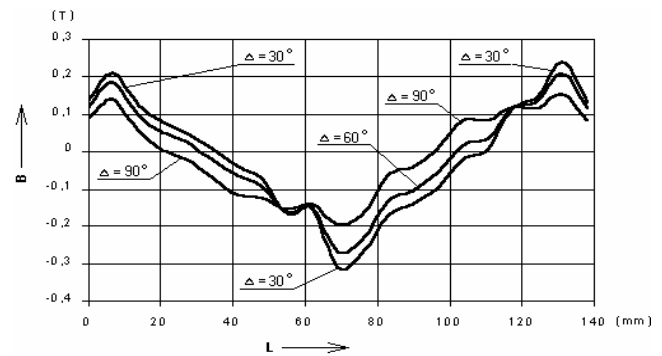


Fig. 3. Magnetic flux density distribution under the inductor when there is different current phase time shifts in the windings at 0.83 ms from starting time

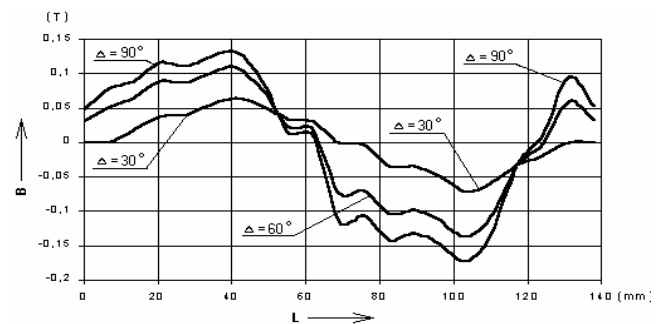


Fig. 4. Magnetic flux density distribution under the inductor when there is different current phase time shifts in the windings at 5.83 ms from starting time

It is also evident that in the presence of different current shift in phase in the windings, the amplitudes of the magnetic flux density fluctuations differ.

Simulation of flux density under different tooth's (Fig. 5) shows, that magnetic field under ending and middle tooth pulsates with different amplitudes and phases, but frequencies are same.

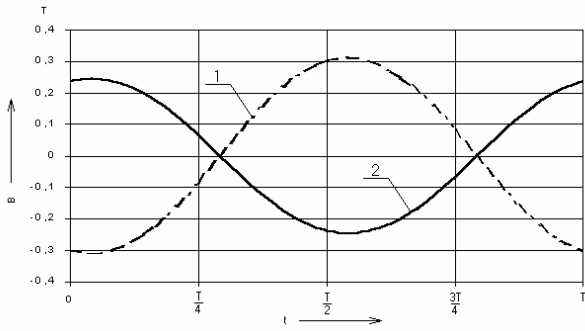


Fig. 5. Flux density's changes under ending and middle tooth of inductor: 1 – under middle tooth, 2 – under ending tooth

Comparing flux density distribution in different cross-section's (Fig. 6) it can be seen, that flux density varies along, and across the air gap. This can be explained by tooth top leakage effect.

Fig. 7 shows how varies the magnetic flux outside inductor at different instants of time. Magnetic flux are changing periodically, growing to maximum value and reducing to zero. Receding from inductor ends magnetic flux is reducing by exponent [4]. By comparing magnetic flux at same time moment in both sides of inductor, it is possible to see, that the magnetic flux outside the right end of inductor is a little bit stronger, than the magnetic flux outside left end of inductor.

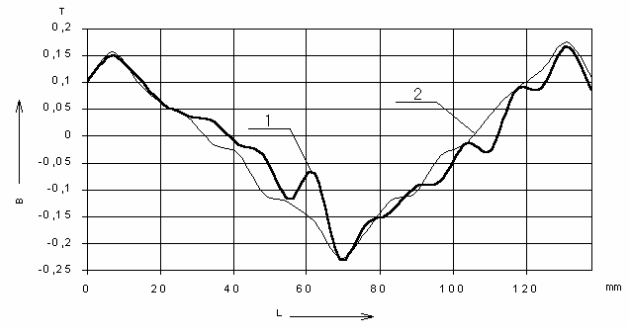


Fig. 6. Flux density distribution in different cross-sections of the air gap: 1 – cross-section near inductor, 2 – cross-section near secondary element

It is noteworthy that the magnetic flux density (in case of single-phase LCM) outside the inductor ends depends on time instant and value of current shift in phases (Fig. 8). Magnetic flux outside the left end of inductor is a little bit stronger, than the magnetic flux outside right end of inductor.

By investigating magnetic flux outside the inductor at different air gap widths (Fig. 9) it is possible to see, that characteristic are not linear: then is big air gap width, when dependency on air gap width changing is lower [5].

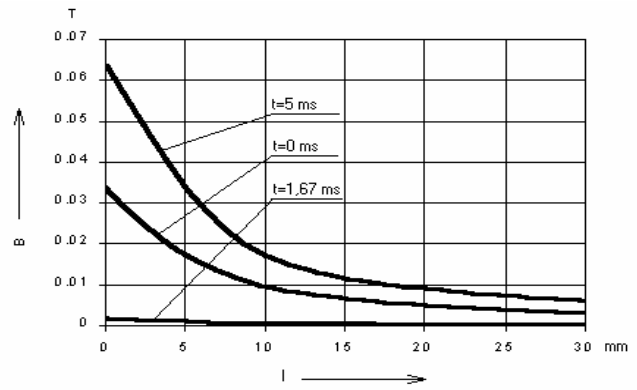
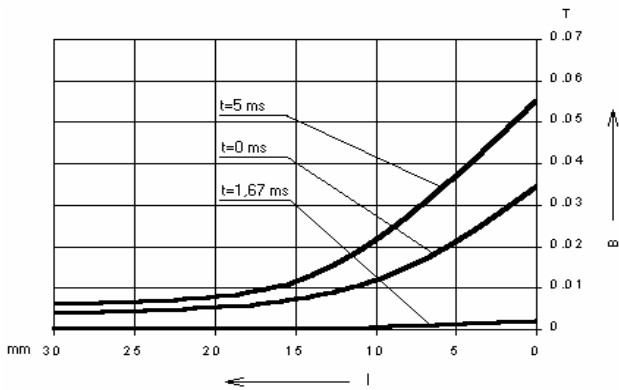


Fig. 7. The distribution of magnetic flux density outside inductor at different instants of time

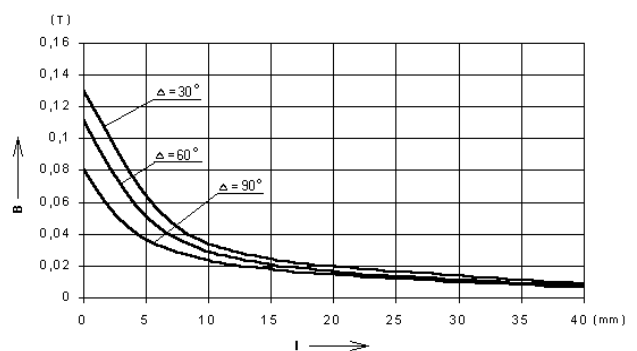
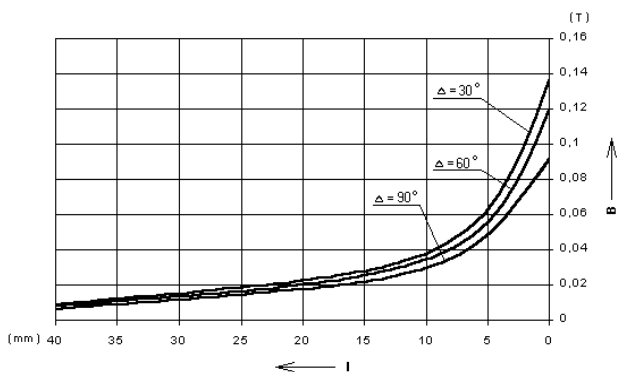


Fig. 8. The distribution of magnetic flux density outside of the inductor ends with different current shifts in phases at 0.83 ms from starting time

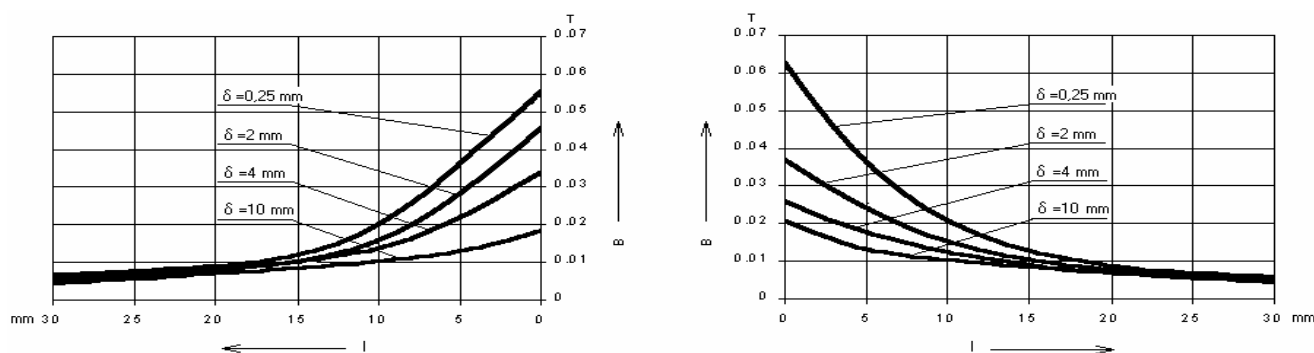


Fig. 9. The distribution of magnetic flux outside inductor at different air gap widths δ

Conclusions

1. The distance at which magnetic flux density outside inductor ends is equal to zero depends on the instantaneous value of magnetic flux density in the ending tooth of the inductor.

2. As the current phase time shift differences change, the amplitude of the magnetic flux density (outside the inductor ends) changes dependent on the instant in time.

3. Magnetic flux density in the air gap varieties more in cross-section near inductor then in cross-section near secondary element.

4. Magnetic field under ending tooth varies by the law of sine with the same frequency like under middle tooth of inductor, but lower amplitude. Different between phases of varies depends on parameters of inductor.

References

1. **Boldea, I.** Linear electric actuators and their control. Proceedings of the American Control Conference. – 1997. 2617 p.
2. **Jin, J.** The finite element method in electromagnetics. – 2002. – 753 p.
3. **Monk P.** Finite Element Methods for Maxwell's Equations. – 2003. – 336 p.
4. **Smilgevičius A., Sadauskas T.** Simulation of magnetic field of linear asynchronous motor // Electrical and Control Technologies. Proceedings of International Conference. – 2006. – 125 p.
5. **Sadauskas T., Smilgevičius A.** Simulation of magnetic field of single-phase linear capacitor motor // Doctoral school of energy- and geo-technology. 4th International Symposium. – 2007. – 177 p.

Submitted for publication 2007 02 27

T. Sadauskas, A. Smilgevičius, Z. Savickienė. Distribution of Magnetic Field of Linear Induction Motor // *Electronics and Electrical Engineering*. – Kaunas: Technologija, 2007. – No. 4(76). – P. 63–66.

In this article is investigated the distribution of magnetic field of linear induction motor. There are two models for simulation: three-phase asynchronous linear motor and single-phase linear capacitor motor. Simulation results of asynchronous LIM at different instants of time and at different widths of air gap are presented. There are given results of simulation, which show the change of magnetic flux at different instants of time of linear capacitor motor how magnetic field varies at different instants of time and at different current shifts in phases. Charts of magnetic flux density below ending and middle tooth of inductor, and magnetic flux density in different cross-sections of air gap are compared. Ill. 9, bibl. 5 (in English; summaries in English, Russian and Lithuanian).

T. Садаускас, А. Смильгявичус, З. Савицкене. Распределение магнитного поля в линейном двигателе // *Электроника и электротехника*. – Каунас: Технология, 2007. – № 4(76). – С. 63–66.

Исследуется распределение магнитного поля в линейном двигателе. Рассматриваются две модели – трёхфазный асинхронный линейный двигатель и однофазный конденсаторный линейный двигатель. Представлены графики распределения плотности магнитного потока асинхронного линейного двигателя в воздушном зазоре и за концами индуктора в разные моменты времени и при разной величине воздушного зазора. Изображены распределения плотности магнитного потока однофазного конденсаторного линейного двигателя в разные моменты времени при наличии нескольких разных фаз тока в обмотках. Рассмотрены временные изменения плотности магнитного потока под последним и средним зубцами индуктора, а также распределение магнитного поля в разных местах сечения воздушного зазора. Ил. 9, библи. 5 (на английском языке; рефераты на английском, русском и литовском яз.).

T. Sadauskas, A. Smilgevičius, Z. Savickienė. Tiesiaeigio variklio magnetinio lauko pasiskirstymas // *Elektronika ir elektrotechnika*. – Kaunas: Technologija, 2007. – Nr. 4(76). – P. 63–66.

Tiriamas magnetinio lauko pasiskirstymas tiesiaeigiame variklyje. Nagrinėjami du modeliai – trifazis asinchroninis tiesiaeigis variklis ir vienfazis kondensatorinis tiesiaeigis variklis. Pateikti asinchroninio tiesiaeigio variklio magnetinio srauto tankio oro tarpe ir už induktoriaus galų pasiskirstymo grafikai skirtingais laiko momentais bei esant skirtingiems oro tarpo dydžiams. Pavaizduoti vienfazio tiesiaeigio kondensatorinio variklio magnetinio srauto tankio pasiskirstymai skirtingais laiko momentais bei esant kelioms skirtingoms srovių fazėms apvijose. Nagrinėjami magnetinio srauto tankio laikiniai kitimai po galiniu bei viduriniu induktoriaus dantimis bei magnetinio lauko pasiskirstymas skirtinguose oro tarpo pjūviuose. Il. 9, bibl. 5 (anglų kalba; santraukos anglų, rusų ir lietuvių k.).

DOI: 10.5755/j02.eie.10721